HHS Public Access

Author manuscript

Langmuir. Author manuscript; available in PMC 2018 August 09.

Published in final edited form as:

Langmuir. 2016 February 23; 32(7): 1909–1919. doi:10.1021/acs.langmuir.5b04314.

Quantifying Drug-Induced Nanomechanics and Mechanical Effects to Single Cardiomyocytes for Optimal Drug Administration To Minimize Cardiotoxicity

Tao Yue[†], **Ki Ho Park**[‡,§], **Benjamin E. Reese**[†], **Hua Zhu**[‡,§], **Seth Lyon**[†], **Jianjie Ma**[‡,§], **Peter J. Mohler**[‡], and **Mingjun Zhang**[*,†,‡,∥]

[†]Department of Biomedical Engineering, The Ohio State University, Columbus, Ohio 43210, United States

[‡]Dorothy M. Davis Heart & Lung Research Institute, The Ohio State University Wexner Medical Center, Columbus, Ohio 43210, United States

[§]Department of Surgery, The Ohio State University Wexner Medical Center, Columbus, Ohio 43210, United States

[∥]Interdisciplinary Biophysics Graduate Program, The Ohio State University, Columbus, Ohio 43210, United States

Abstract

Contrary to the well-studied dynamics and mechanics at organ and tissue levels, there is still a lack of good understanding for single cell dynamics and mechanics. Single cell dynamics and mechanics may act as an interface to provide unique information reflecting activities at the organ and tissue levels. This research was aimed at quantifying doxorubicin- and dexrazoxane-induced nanomechanics and mechanical effects to single cardiomyocytes, to reveal the therapeutic effectiveness of drugs at the single cell level and to optimize drug administration for reducing cardiotoxicity. This work employed a nanoinstrumentation platform, including a digital holographic microscope combined with an atomic force microscope, which can characterize cell stiffness and beating dynamics in response to drug exposures in real time and obtain time-dose-dependent effects of cardiotoxicity and protection. Through this research, an acute increase and a delayed decrease of surface beating force induced by doxorubicin was characterized. Dexrazoxane treated cells maintained better beating force and mechanical functions than cells without any treatment, which demonstrated cardioprotective effects of dexrazoxane. In addition, combined drug effects were quantitatively evaluated following various drug administration protocols. Preadministration of dexrazoxane was demonstrated to have protective effects against doxorubicin, which could lead to better strategies for cardiotoxicity prevention and anticancer drug

[*]**Corresponding Author:** zhang.4882@osu.edu.

ASSOCIATED CONTENT

Supporting Information

The Supporting Information is available free of charge on the ACS Publications website at DOI: 10.1021/acs.langmuir.5b04314. Primary mouse cardiomyocytes, spontaneous and electric stimulated contractions, base line nanomechanics characterization, cardiomyocyte selection criteria, DHM phase time-dependent monitoring of the region of interest, multipeak analysis for AFM "dwell" curve, and shape changes of cardiomyocytes during experiments (PDF)

The authors declare no competing financial interest.

administration. This study concluded that quantification of nanomechanics and mechanical effects at the single cell level could offer unique insights of molecular mechanisms involved in cellular activities influencing organ and tissue level responses to drug exposure, providing a new opportunity for the development of effective and time-dose-dependent strategies of drug administration.

Abstract

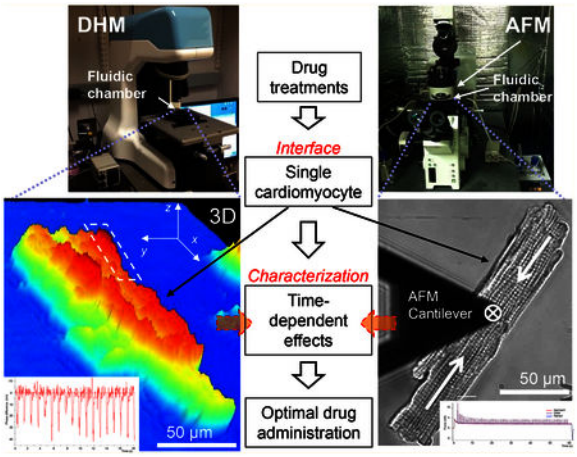

INTRODUCTION

Cardiac diseases may be caused by chemical and physical or mechanical stresses to cardiomyocytes.[1] Among the deleterious effects, the cardiotoxicity caused by anticancer drugs is a major concern.[2,3] While much work has been conducted to analyze cardiac dynamics and mechanics at the organ and tissue levels, the mechanisms of cardiotoxicity are still under investigation because of the complexity of relevant factors involved at the macroscale.[4,5] Consequently, there is a lack of an effective approach in current clinical practices to directly correlate drug effects with cellular functions and optimize drug administration through the minimization of cardiotoxicity.[6–8] It remains a daunting challenge to understand the cellular mechanics associated with cell functions and clinical interests, such as optimal dosage and time-dependent administration of multiple drugs.[5,9] According to previous studies, single cell nano-mechanics and mechanical properties are necessary for revealing underlying mechanisms and drawing direct correlations with cellular functions to understand pathophysiology at the organ level.[10–12] Nanoscale characterization is able to explore quantitative information on single cells and subcellular activities and uncover potential pathways directly related to diseases and treatment strategies.[13–16] Understanding dose and time-dependent effects of drugs is critical for improving drug administration, for maximizing therapeutic effects and mitigating potential side effects.[17] Drug-induced changes on nano-mechanics and mechanical properties of single cardiomyocytes may also provide direct evidence of these effects.[18] An atomic force microscope (AFM) is capable of directly measuring both material and mechanical properties of single cells.[19–21] However, the tip—surface interactions that occur during contact measurements could induce undesirable side effects to soft biological samples. Alternatively,

a digital holographic microscope (DHM) can be used to conduct noncontact and noninvasive three-dimensional (3D) characterization.[22,23] Its applications at the single cell level have shown advantages for investigating cell dynamics and biological events.[24–26] DHM provides quantitative phase data that can be used to reveal material and morphological information, which may not be obtained under conventional optical observations when detecting only the intensity component of light.[27,28]

Doxorubicin is an anthracycline anticancer drug with cardiotoxic side effects, which result in apoptosis of cardiomyocytes and cardiac injury.[4,29,30] Most studies about the mechanisms involved in doxorubicin-induced cardiotoxicity have focused on the long-term (months to years) effects taking place at the organ level, which have not been shown very effective in revealing underlying mechanisms or developing optimal cardioprotective strategies.[31,32] Dexrazoxane is a cardioprotective agent with proven efficacy on preventing cardiotoxicity in cancer patients receiving anthracycline chemo-therapy. However, the exact mechanisms of its cardioprotective effects are still not fully investigated.[33,34] Effective clinical usage and resulting evaluation of dexrazoxane during anthracycline administration are highly expected.[35] Time-dependent characterizations of cellular mechanics may provide a direct way to evaluate and understand drug-induced effects.[36]

This work presents a DHM/AFM integrated nanoinstrumentation platform and approach for single cell characterization, while maintaining precise control over the micro-environment. As shown in Figure 1, the platform includes a newly developed DHM to perform noncontact and real-time 3D nanoscale imaging. An AFM is used to apply and measure forces to/from single cardiomyocytes relating to the cell surface/membrane. Both contact and noncontact nanocharacterization have been performed along with direct comparisons made between samples. Comparing to studies with focus on one mechanical effect,[36,37] this research integrated cell stiffness, beating pattern, and force to uncover the underlying nanomechanics of single cardiomyocytes. This complementary platform is able to provide robust and comprehensive data for quantifying single cell mechanics. The cardiomyocytes are placed in a closely controlled microfluidic chamber that can be transferred between the microscopes. Using this platform, a wide array of parameters of nanomechanics in response to the exposures of anticancer drugs has been obtained. We found that doxorubicin-induced cardiotoxicity included an acute increase, followed by a delayed decrease of surface beating force. Cardioprotective effects of dexrazoxane were evaluated in terms of mechanical function at the single cell level. Prevention of doxorubicin-induced cardiotoxicity was evaluated following various dexrazoxane administration strategies, which could help establish direct indications of drug effects, and eventually improve current cardiotoxicity prevention strategies. Preadministration of dexrazoxane mitigated the initial mechanical stress induced by doxorubicin and helped prevent acute cell damage. This study provides a promising way to reveal clinically relevant mechanical effects and evaluate the effects of various clinical treatment strategies.

EXPERIMENTAL SECTION

Experimental Procedures.

Primary mouse cardiomyocytes were isolated from wild-type mice and used as samples in the experiments (detailed isolation procedures are described in the Supporting Information). The experiments were conducted in six groups. The control group is under normal culture condition without any drugs. The cases treated by one type of drug include the doxorubicin (Cayman Chemical Co.) treated group and the dexrazoxane (Sigma-Aldrich) treated group. Different administration protocols of two drugs include the administration of both drugs at the same time, the administration of doxorubicin 30 min before dexrazoxane, and the administration of dexrazoxane 30 min before doxorubicin. In each case, the concentrations of doxorubicin and dexrazoxane were 10 μM and 20 μM, respectively. The cardiomyocytes were continuously monitored by DHM or AFM for about 2 h. The temperature inside the fluidic chamber was maintained at 37 °C. Both the static (cell stiffness) and dynamic (surface beating force and beating duration) data were acquired every 10 min during each experiment for a total of 90 min.

A total of 24 mice were used to gather data. Four mice were used in each group. Experiments were performed by collecting beating dynamics using DHM and AFM while doxorubicin and dexrazoxane were exposed to the cells *in vitro.* Primary mouse cardiomyocytes were isolated from adult wild-type mice and immediately placed in the environmental chamber to maintain adult morphology and minimize the effects of long-term culture. Primary mouse cardiomyocytes are typically quiescent or can have unpredictable spontaneous activity. Due to the variability in the range of forces produced from cell to cell, and the inconsistencies in beating frequency, using an electrical stimulator to induce contractions was able to remove some of the inconsistencies by generating a much more stable response. Controlled stimulation also provides a stable beating pattern from the desired cells to facilitate the data acquisition, while the spontaneous beating is unpredictable. More details are described in Supporting Information Figure S1.

Because the real mechanical properties of individual cells are mainly influenced by the growth conditions of the mice, isolation techniques, and other random parameters, there are significant variations of mechanical properties between cells. To remove variations and allow comparisons to be made between cells, we developed a systematic approach to select cells and process data, which included the cardiomyocyte selection criteria, data acquisition, optimization, and analysis protocols.

Regarding cardiomyocyte selection, the investigation of whether size could be used to predict the relative beating force was first performed. Two spontaneously active cells, including a relatively smaller one and a larger one, were placed side by side in a Petri dish. Each cell was monitored using the AFM in order to compare the average beating force in response to variable loading conditions. The beating force was measured by AFM according different cell size and sarcomeric organization, to determine the proper cells used for acquiring data. More details are described in Supporting Information Figure S3.

Surface beating data were collected as force versus time, with indentations being acquired at set intervals between beating data sets. Beating data were collected at 60 s dwell intervals, and the cantilever was retracted between every data set. Stimulation was turned off between every dwell in order to ensure a reproducible contact force on the cell surface. Time-course data were extracted from the “dwell” portion of dwell curves performed by AFM measurements. The optimization was performed using a multipeak analysis package in the Igor software (Igor Ver.6.34, WaveMetrics, Inc.). The last 30 peaks were much more stable. They are selected and fit individually to analyze the observed beating dynamics including the surface beating amplitude and duration full width at half-maximum (fwhm). More details are described in Supporting Information Figure S5. For DHM, the cell beatings were recorded and processed by Koala software (V4, Lyncee Tec), More details are described in Supporting Information Figure S4. The surface height changes of contractions were calculated as shown in Figure 2. Both DHM and AFM data were summarized, and then the statistical averaging was done on each data set.

The time for each experiment was approximately 2 h, and cells were only used within 6 h after isolation, as it has been shown that changes can begin to occur after this time period which alter the cardiomyocyte morphology and could obscure the resulting data. At least 10 min of stable measurements were collected, and then drugs were added to the sample without altering the positioning of the AFM tip on the cell, or the cell position on DHM. Both control and drug treated samples were examined under identical settings and conditions for the same period of time, after which data were then combined and averaged for each group. Finally, the normalized data for each cell were used to generate relative values for all of the parameters measured.

Digital Holographic Microscopy Measurement.

In order to obtain the real-time cell morphological changes as well as to prevent the influences from AFM contact measurement on cell membrane, DHM (T1000, Lyncee Tec) was utilized as a noninvasive, noncontact, and real-time 3D measurement for single cardiomyocytes. DHM uses a CCD camera to record a hologram which is then transmitted to a computer in order to digitally reconstruct the image in 3D. Real-time cellular dynamics and time-course data can be recorded using this noninvasive technique of DHM. The hologram is formed by combining intensity and phase information. Cell 3D morphological data and intracellular refractive index are contained in the phase images.[27] Based on the Koala software (V4, Lyncee Tec), real-time quantitative phase monitoring can be accomplished. The ability to monitor phase changes over time allows data to be extracted and analyzed. A data postprocess program was coded by MATLAB for calculating the maximum surface beating area (the contraction center) for each individual contraction. Two analysis approaches were utilized as shown in Figure 2.

First, 1D phase profile data across the maximum surface beating area were used to calculate the quantitative height change during the contraction. This provides the measurement of cell height information along the desired profiling line. However, it is hard to have a comprehensive description of the contraction center region, because the cell contraction center is not only a single point but a certain region with periodic activities. Second, a 2D

region of interest (ROI) covering the maximum surface beating area was defined in the phase image. In Koala software, the topographic information is obtained in a time-dependent manner, including the detail height distribution and mean value of the defined ROI. Both 1D and 2D height data indicate the cell surface beating amplitude and are correlated with the AFM measurement data. By monitoring phase changes of ROI in real-time, cell beating duration (fwhm) was also obtained by monitoring phase changes of ROI frame by frame, as shown in Supporting Information Figure S4.

Atomic Force Microscope Measurement.

In order to determine the cell stiffness for a given sample, a technique termed nanoindentation was performed on the cell's surface, utilizing the AFM (MFP-3D SPM, Asylum Research). This technique produces force curves that can then be further analyzed using Hertz theory to calculate a measure of elasticity or stiffness for individual or aggregated cells.[20] As the cantilever tip contacts the sample, the interaction between the two surfaces produces a force curve (force versus distance) from which the slope of this curve can then be used to quantify the stiffness of the sample.

Triggered force curves allow the user to define the maximum force with which to apply on the sample before the cantilever is retracted. This allows for more consistency when combining data from several samples and also minimizes the amount of damage to both the sample and the cantilever tip. By defining a trigger force of 1 nN, the AFM cantilever would then approach the surface at a given velocity over a predefined distance until contact is made and the deflection signal reaches a value equal to 1 nN of force. The tip geometry and its material properties are very important for accurately representing the interaction between the AFM cantilever and the cell's surface. For the purposes of this work, a spherical tip (with 2 μm in diameter) was used in order to remove some of the variability and difficulties in the calculation of cell stiffness, which comes from using more complex geometries. By using a spherical tip, this also ensures a more uniform and reproducible interaction without causing damage to the cell, which can sometimes be a problem when using a sharp tip on soft biological samples. Another important consideration is the stiffness of the cantilever relative to the sample. Using a softer cantilever provides more sensitivity over a lower range of expected force values (1–100 nN). This also minimizes the damage that might occur to the cell's surface by using a relatively low spring constant cantilever (0.02–2 N/m).

Once the force curves were acquired, a built-in software package was used to extract the desired parameters of interest. Depending on the sample and the design of the experiment, the contact portion of the force curve can be fitted over a specific region of interest. The stiffness can therefore be determined over a confined range of either force or indentation depth. A range of force curves were performed in order to ensure that the correct force and indentation depth were being used to remove any unwanted influences from the underlying substrate. In order to acquire cardiomyocyte dynamics regarding beating capability (surface beating force) and the associated beating parameters (beating duration fwhm), a technique similar to that previously described was utilized. This technique was used on spontaneously or stimulated activated cardiomyocytes in order to generate a "dwell map", showing spatial

variations in the acquired parameters. Measurements were taken from a single point on the cell's surface (center of beating) and are referred to as a dwell curve.

Electrical Stimulation.

A Grass SD9 neurophysiological stimulator was used to generate short pulses while connected to platinum stimulation electrodes submerged within the environmental chamber housing the isolated cardiomyocytes. Depending on a combination of parameters from the experimental setup, which includes the stimulation frequency, voltage, pulse delay, and duration, the minimum threshold voltage and pulse duration was found to induce contractions while minimizing the effects and disturbances to the cells. The parameters were set to 1 Hz of stimulation frequency, 0.1 ms of pulse delay, and 5 ms of pulse duration. For different mice and cells, the excitation threshold voltage was different. In our experiments, 10–30 V of voltage was used. Electrical stimulation was given to the cell once every 10 min during the whole experiment. Each of stimulations lasted 60 s to obtain the stable beating pattern.

Statistical Analysis.

All data were expressed as mean ± sem (standard error of the mean). Statistical analysis was used at each time point for comparison among different data sets. Prism 6 (GraphPad) software was used for statistical analyses to determine the statistical significance between samples at each time point. For comparison between two groups which had unequal population variances, an unpaired two-tail Student's t test with Welch's correction was performed. For other comparison among two or more treatment groups, one-way ANOVA followed by Tukey's posttest was performed.

RESULTS AND DISCUSSION

Quantifying Nanomechanics and Mechanical Effects of Single Cardiomyocytes.

Figure 2 shows a typical setup for characterizing contraction dynamics of single cardiomyocytes using DHM. Stimulated contractions are recorded as time-course data. The phase information can be used to calculate cell thickness. The contractions act in short time, and the reflective index of the cell is considered without significant changes during such short time. The phase difference is linearly correlated with cell thickness. Therefore, phase images can be used to calculate the height change during each contraction, which indicates the cell's surface beating amplitude, and to be correlated with the AFM data. Figure 2a shows the phase images of single cell contraction, including a relaxed status and the maximum contracted time status. By comparing the two images, the maximum surface beating area representing the contract center was calculated and visualized as shown in Figure 2b. A ROI covering this area and reflecting the most significant surface change was defined, as shown in Figure 2a. As a 1D characterization approach, a profile line across the ROI can be further defined, and the quantitative height profiling has been shown in Figure 2d. The height change Δh is then used to represent the surface beating amplitude. In addition to phase changes over the defined line from within the ROI, information was obtained in a time-dependent manner over the entire area defined within the ROI. As shown in Figure 2e, representative time-course data can be obtained to calculate the surface changes during each

contraction cycle. Two-dimensional ROI characterization for the maximum surface beating area can be more useful than the localized AFM probing for the beating dynamics. By monitoring the phase changes of the ROI in real time, cell beating duration, which is called fwhm, can be obtained, as shown in Supporting Information Figure S4.

Figure 3 shows a typical setup for AFM characterization of single cardiomyocytes. The data set obtained includes cell stiffness, surface beating amplitude/force ,and fwhm. Figure 3a shows the measurement point of an AFM cantilever on a cell body. The center of contraction was defined as the largest contraction force value measured over the surface of the cell. Based on the initial force curve when contacting the cell, the cell stiffness was characterized, and a representative data set is shown in Figure 3b. The cantilever approached and then deformed the cell membrane. As the cantilever position lowered, the indentation force increased. As shown in Figure 3c, an initial decay can be seen upon the initiating stimulation, and then the beating level decreased to a stable value after about 30 s. The last 30 peaks are more stable than the initial 30 peaks. These last 30 peaks are selected and fitted to evaluate the beating capability and pattern of individual cells.

Time-dependent nanomechanics obtained by our platform can be used to reveal cellular functions and conditions and establish a bottom up model to correlate activities at the tissue and organ levels. In response to drug exposures and environmental changes, the mechanical properties of single cells are supposed to change.[38] A force measurement platform was presented to characterize the contractility of single cardiomyocytes.[39] However, the platform lacks direct cell stiffness measurement that is very important for understanding nanomechanics of single cells. The change of cell stiffness may indicate the changes of protein and lipid orientations within and/or underneath the plasma membrane.[40,41] This change reflects the effects of drug treatments, physical wounding, and changes of the microenvironment. Stiffness can also be used to derive various cell states or conditions,[15,42] while cell beating force can directly reflect the performance capabilities of cardiomyocytes as they relate to cardiac performance in response to drug administration.[43]

As described in Supporting Information Figure S1, the stimulation is indispensable for obtaining a stable beating pattern. We first characterized the time-course changes of cell stiffness, beating force, and fwhm during 90 min experiments without any drug treatment to evaluate the effects of electric stimulation. Results are shown in Supporting Information Figure S2. These data then served as a baseline condition for comparing with the drug treated groups.

Doxorubicin-Induced Cardiotoxicity and Dexrazoxane-Mediated Cardioprotective Effects.

Figure 4a shows the stiffness versus time data, one of the properties relating to cellular nanomechanics having a response to single drug treatment. The relative stiffness for the cardiomyocytes treated with doxorubicin showed an initial increase of about 25% over the first 50 min of exposure, matching control samples. The relative stiffness for these cells then dropped back to a stable value close to its initial range for the remainder of their exposure. However, control samples maintained a relatively steady average increase over time, peaking at about 40% higher than initial values when measurements were stopped at 90 min. This demonstrates the possibility of a threshold effect induced by doxorubicin regarding cell

stiffness after about 60 min of exposure. The relative stiffness of samples treated with dexrazoxane decreased less than 10% at about 40 min, then followed a similar trend as the control samples, having a gradual increase. Relatively speaking, the dexrazoxane treated cells had only slightly lower values throughout their 90 min of exposure, indicating that dexrazoxane might not have any significant effects on cell stiffness.

Figure 4b shows the fwhm versus time data. Control samples had a relatively stable fwhm with a slight fluctuation occurring between 70 and 80 min but were able to maintain values similar to those of the initial measurements by the end of the experiment. After about 20 min, the fwhm of doxorubicin treated samples increased gradually and finally reached values 15% higher than the control, which indicated a longer beating duration. fwhm of dexrazoxane treated samples decreased about 10% in the first 10 min and then maintained a significantly lower level than the control, with a gradual increase after 70 min.

The surface beating force versus time data are shown in Figure 4c. After doxorubicin treatment, the relative beating force had an acute increase of about 20% after 20 min of exposure, followed by an eventual decrease to about 40% of the initial values. Control samples maintained a relatively slower rate of decline throughout the course of the experiment. Eventually, the doxorubicin treated group exhibited significantly lower forces than control samples. The force of dexrazoxane treated cardiomyocytes maintained a relatively stable level compared with initial values and remained at a higher value than the control cells after 90 min, demonstrating the possible cardioprotective effects of dexrazoxane in cardiomyocytes.

Based on the aforementioned single drug-induced effects, there is a time-dependent correlation between the drug effects and the measured mechanical properties of single cells, leading to a better understanding of the ways in which single cell mechanics can be associated with important cellular functions of clinical interest. Biochemical assays to study cardiomyocyte contraction have been established through investigating Ca^{2+} ion changes.[44,45] However, the contractility is derived through its correlation with ion concentrations, which has that limited accuracy. On the contrary, our platform provides direct information about the force and stiffness changes during the drug treatment, which mitigates the influence from irrelevant metabolism products or other environmental ion changes, and provides more accurate information.

In the doxorubicin treated group, the initial acute increase in the force response of cardiomyocytes was thought to be associated with doxorubicin exposure. The acute increase in beating force, however, might be caused by the mechanical stress induced from doxorubicin, which in turn has been shown to compromise cellular functions and result in apoptosis.[46] These findings were obtained based on our real-time single cell nanomechanics monitoring, which was more advanced than previous research studies which could not confirm whether an increase or no change in contractility occurs in response to doxorubicin.[47] Interestingly, prolonged treatment with doxorubicin resulted in decreasing surface beating force and lower stiffness in comparison with control, which might explain the long-term pathological damage seen *in vivo* in both animal studies and human patients. We believe that the time-dependent response of cardiomyocytes might correlate with the intramyocardial

metabolism of doxorubicin to doxorubicinol as well as the long-term effects seen in patients receiving treatment.[48] Thus, the stiffness decrease might be related with the damage caused by doxorubicin. The long-term response could also point toward the increased accumulation and production of the major metabolite doxorubicinol within the cell. The time delay decrease might show the metabolism process of doxorubicin and potential thresholds for indicating cardiotoxicity.

Furthermore, the electric stimulation might cause the cell function deterioration during 90 min experiments as observed in the control group. This might be the result of a gradual increase of calcium ions over time due to potential electro-poration or damage to the cell membrane. Interestingly, dexrazoxane treatment maintained the cell beating force level throughout the whole experimental period. One explanation might be that dexrazoxane diffuses into cells and hydrolyses to an EDTA-like diacid-diamide, and chelates ions and inhibits the formation of superoxide radicals within the environment, which may directly affect cellular mechanical properties.[8]

Dexrazoxane and Doxorubicin Combined Effects: Optimize Drug Administration Strategy.

The combined effects of doxorubicin and dexrazoxane under different administration protocols were evaluated. These protocols included the following: administration of both drugs at the same time, 30 min earlier of doxorubicin administration than dexrazoxane, and 30 min earlier of dexrazoxane administration than doxorubicin, which are abbreviated as “same time”, “Dox2013Dex”, and “Dex–Dox”, respectively, in the following content and figures.

Figure 5a shows the time-course data for cell stiffness of all groups. In the same time group, the relative stiffness decreased about 15% in 20 min and then showed a gradual increase back to a similar level when compared with control samples. In the Dox–Dex group, after dexrazoxane was introduced, the relative stiffness decreased 20% within 10 min and then quickly increased, reaching values similar to control samples. Finally, in the Dex–Dox group, after doxorubicin was introduced, the relative stiffness for treated samples decreased about 15% and then remained relatively stable for the remainder of the experiment, having a much lower value compared to the other groups.

The fwhm versus time data of all groups are shown in Figure 5b. In the same time group, the fwhm dropped over the first 50 min and then increased quickly, finally reaching about 20% higher than control. In the Dox–Dex group, the fwhm maintained a stable level in the first 60 min and then had an acute increase about 25% until the end of the experiments. With respect to the Dex–Dox group, it had a significantly lower fwhm than the other drug treated groups after 50 min, with a gradual increase after 70 min. Eventually it reached almost the same value of control. From the stiffness and fwhm data, the Dex–Dox group shows a significant difference after about 50–60 min in comparison with other groups, which showed the existing cellular mechanical properties difference.

Figure 5c shows the beating force data of all groups. In the same time group, the administration of dexrazoxane mitigated the acute increase of the beating force in the first 20 min. However, it was followed by a constant decrease and the final value of force was about

60% of the original level. Consequently, the acute damage was not prevented by this drug administration approach.

In the Dox–Dex group, the drug treated samples had a 20% acute increase after 20 min; however, a higher beating force was sustained until 50 min after drug exposure, much longer than the doxorubicin treated group (30 min). This showed that the acute damage caused by the mechanical stress induced after doxorubicin exposure had longer lasting effects, which were more harmful to the cells. This resulted in the quick decline of beating force after 60 min and resulting lower level after 90 min. This showed that the acute damage might be irreversible and could not be fully repaired through delayed dexrazoxane administration, which also indicated that this damage might permanently influence the mechanical properties of these cells.

With respect to the Dex–Dox group, the administration of doxorubicin after 30 min still caused a force increase less than 10%, lower than previous cases. Then the force maintained a relatively stable value. After 90 min, the treated samples still remained 10% higher than other groups. It demonstrated that the acute damage was mitigated by the preadministrated dexrazoxane.

Based on the aforementioned drug-combined effects, we found different levels and periods of beating force peak according to different drug administration strategies. We correlated the changes of single cell mechanics and mechanical properties with different drug administration protocols and demonstrated the possibility to optimize the clinical drug administration strategies. The earlier dexrazoxane administration had the shortest and lowest peak period compared with the other two groups. It showed that the preadministration of dexrazoxane might prevent the doxorubicin's acute stress response. The other two administration approaches of dexrazoxane did not show significant cardioprotective effects in terms of beating force level. These results suggested that administration sequence should be considered as one of the important factors in clinical usage.[7,17,49,50]

All dexrazoxane-combined cases had a higher force level after 90 min compared with the doxorubicin-only treated group. This showed that dexrazoxane treated cells maintained better beating capabilities, both in terms of beating force and duration. These effects may demonstrate the iron-chelating function of dexrazoxane through its rapid metabolism, which prevents oxidative stress, mitigates the induced toxicity, and further protects the cells.[50,51] The force level difference can be used as an indicator to improve drug administration strategies in cancer treatments, including the clinical dosage and drug administration sequences.

Additionally, DHM has the potential to provide further insights for single cells beyond the current properties and applications illustrated in this study. The refractive index of cells obtained through phase data collection is related with intracellular molecular concentrations and other values of interest.[52] Further applications may include the analysis of biological events such as cell division and cell death characterization, and their correlations with cell 3D morphological information.[24,26]

CONCLUSIONS

The integrated DHM/AFM nanoinstrumentation platform was demonstrated to be capable of quantitatively characterizing the mechanobiological properties of single cardiomyocytes in response to the exposures of doxorubicin and dexrazoxane. At the single cell level, we explored the mechanisms of doxorubicin-induced cardiotoxicity and dexrazoxane-mediated cardioprotective effects. The acute increase of surface beating force induced by doxorubicin was newly quantified. This initial increase revealed the damage caused by the mechanical stress induced by the drug, and the time-delayed decrease showed that the toxicity originating from the accumulation of resulting metabolites came at a later stage. Cells maintained beating force levels and mechanical functions with dexrazoxane treatment. At the single cell level, preadministration of dexrazoxane was found to have better cardioprotective effects, which could contribute to the improvement of cardiotoxicity prevention and anticancer drug administration protocols. Beyond the aforementioned experiments, this approach also demonstrates the high level of flexibility provided by using various drug types, administration timing, and dosage. This will contribute to the development of more effective treatment strategies for various treatments and will help in understanding the therapeutic effectiveness of drugs.

Supplementary Material

Refer to Web version on PubMed Central for supplementary material.

ACKNOWLEDGMENTS

This work was supported by the Startup Fund from the Department of Biomedical Engineering of The Ohio State University.

REFERENCES

(1). Maillet M ; van Berlo JH ; Molkentin JD Molecular basis of physiological heart growth: Fundamental concepts and new players. Nat. Rev. Mol. Cell Biol 2013, 14, 38–48.23258295

(2). Albini A ; Pennesi G ; Donatelli F ; Cammarota R ; De Flora S ; Noonan DM Cardiotoxicity of Anticancer Drugs: The Need for Cardio-Oncology and Cardio-Oncological Prevention. J. Natl. Cancer Inst 2010, 102, 14–25.20007921

(3). Brana I ; Tabernero J Cardiotoxicity. Annals of Oncology 2010, 21, vii173–vii179.20943611

(4). Zhang YW ; Shi JJ ; Li YJ ; Wei L Cardiomyocyte death in doxorubicin-induced cardiotoxicity. Arch. Immunol. Ther. Exp 2009, 57, 435–445.

(5). Lipshultz SE ; Cochran TR ; Franco VI ; Miller TL Treatment-related cardiotoxicity in survivors of childhood cancer. Nat. Rev. Clin. Oncol 2013, 10, 697–710.24165948

(6). Swain SM ; Whaley FS ; Gerber MC ; Ewer MS ; Bianchine JR ; Gams RA Delayed administration of dexrazoxane provides cardioprotection for patients with advanced breast cancer treated with doxorubicin-containing therapy. J. Clin. Oncol 1997, 15, 1333–1340.9193324

(7). de Beer EL ; Bottone AE ; van Rijk MC ; van der Velden J ; Voest EE Dexrazoxane pre-treatment protects skinned rat cardiac trabeculae against delayed doxorubicin-induced impairment of cross-bridge kinetics. Br. J. Pharmacol 2002, 135, 1707–1714.11934811

(8). Hasinoff BB ; Herman EH Dexrazoxane: how it works in cardiac and tumor cells. Is it a prodrug or is it a drug? Cardiovasc. Toxicol 2007, 7, 140–144.17652819

(9). Vejpongsa P ; Yeh ETH Prevention of Anthracycline-Induced Cardiotoxicity. J. Am. Coll. Cardiol 2014, 64, 938–945.25169180

(10). Cross SE ; Jin Y-S ; Rao J ; Gimzewski JK Nanomechanical analysis of cells from cancer patients. Nat. Nanotechnol 2007, 2, 780–783.18654431

(11). Bryant DM ; Mostov KE From cells to organs: building polarized tissue. Nat. Rev. Mol. Cell Biol 2008, 9, 887–901.18946477

(12). Yue T ; Nakajima M ; Takeuchi M ; Fukuda T Improved Laser Manipulation for On-chip Fabricated Microstructures Based on Solution Replacement and Its Application in Single Cell Analysis. Int. J. Adv. Robot. Syst 2014, 11, 11.

(13). Hansma HG ; Pietrasanta L Atomic force microscopy and other scanning probe microscopies. Curr. Opin. Chem. Biol 1998, 2, 579–584.9818182

(14). Li M ; Liu LQ ; Xi N ; Wang YC ; Xiao XB ; Zhang WJ Nanoscale Imaging and Mechanical Analysis of Fc Receptor-Mediated Macrophage Phagocytosis against Cancer Cells. Langmuir 2014, 30, 1609–1621.24495237

(15). Rother J ; Noding H ; Mey I ; Janshoff A Atomic force microscopy-based microrheology reveals significant differences in the viscoelastic response between malign and benign cell lines. Open Biol 2014, 4, 140046.24850913

(16). Yue T ; Nakajima M ; Takeuchi M ; Hu C ; Huang Q ; Fukuda T On-chip self-assembly of cell embedded microstructures to vascular-like microtubes. Lab Chip 2014, 14, 1151–1161.24472895

(17). Lebrecht D ; Geist A ; Ketelsen UP ; Haberstroh J ; Setzer B ; Walker UA Dexrazoxane prevents doxorubicin-induced long-term cardiotoxicity and protects myocardial mitochondria from genetic and functional lesions in rats. Br. J. Pharmacol 2007, 151, 771–778.17519947

(18). Muller DJ ; Dufrene YF Atomic force microscopy as a multifunctional molecular toolbox in nanobiotechnology. Nat. Nanotechnol 2008, 3, 261–269.18654521

(19). Li QS ; Lee GYH ; Ong CN ; Lim CT AFM indentation study of breast cancer cells. Biochem. Biophys. Res. Commun 2008, 374, 609–613.18656442

(20). Azeloglu EU ; Costa KD Atomic Force Microscopy in Mechanobiology: Measuring Microelastic Heterogeneity of Living Cells In Atomic Force Microscopy in Biomedical Research: Methods and Protocols; Braga PC , Ricci D , Eds.; Humana Press: Totowa, NJ, USA, 2011; Vol. 736, pp 303–329.

(21). Muller DJ ; Dufrene YF Atomic force microscopy: a nanoscopic window on the cell surface. Trends Cell Biol 2011, 21, 461–469.21664134

(22). Cuche E ; Bevilacqua F ; Depeursinge C Digital holography for quantitative phase-contrast imaging. Opt. Lett 1999, 24, 291–293.18071483

(23). Cotte Y ; Toy F ; Jourdain P ; Pavillon N ; Boss D ; Magistretti P ; Marquet P ; Depeursinge C Marker-free phase nanoscopy. Nat. Photonics 2013, 7, 113–117.

(24). Rappaz B ; Cano E ; Colomb T ; Kuhn J ; Depeursinge C ; Simanis V ; Magistretti PJ ; Marquet P Noninvasive characterization of the fission yeast cell cycle by monitoring dry mass with digital holographic microscopy. J. Biomed. Opt 2009, 14, 034049.19566341

(25). Pavillon N ; Kuhn J ; Moratal C ; Jourdain P ; Depeursinge C ; Magistretti PJ ; Marquet P Early Cell Death Detection with Digital Holographic Microscopy. PLoS One 2012, 7, e30912.22303471

(26). Boss D ; Kuhn J ; Jourdain P ; Depeursinge C ; Magistretti PJ ; Marquet P Measurement of absolute cell volume, osmotic membrane water permeability, and refractive index of transmembrane water and solute flux by digital holographic microscopy. J. Biomed. Opt 2013, 18, 036007.23487181

(27). Rappaz B ; Marquet P ; Cuche E ; Emery Y ; Depeursinge C ; Magistretti PJ Measurement of the integral refractive index and dynamic cell morphometry of living cells with digital holographic microscopy. Opt. Express 2005, 13, 9361–9373.19503137

(28). Pavillon N ; Benke A ; Boss D ; Moratal C ; Kuhn J ; Jourdain P ; Depeursinge C ; Magistretti PJ ; Marquet P Cell morphology and intracellular ionic homeostasis explored with a multimodal approach combining epifluorescence and digital holographic microscopy. J. Biophotonics 2010, 3, 432–436.20306502

(29). Takemura G ; Fujiwara H Doxorubicin-induccd cardiomyopathy from the cardiotoxic mechanisms to management. Prog. Cardiovasc. Dis 2007, 49, 330–352.17329180

(30). Carvalho FS ; Burgeiro A ; Garcia R ; Moreno AJ ; Carvalho RA ; Oliveira PJ Doxorubicin-Induced Cardiotoxicity: From Bioenergetic Failure and Cell Death to Cardiomyopathy. Med. Res. Rev 2014, 34, 106–135.23494977

(31). Jones RL ; Swanton C ; Ewer MS Anthracycline cardiotoxicity. Expert Opin. Drug Saf 2006, 5, 791–809.17044806

(32). Kerkela R ; Grazette L ; Yacobi R ; Iliescu C ; Patten R ; Beahm C ; Walters B ; Shevtsov S ; Pesant S ; Clubb FJ ; Rosenzweig A ; Salomon RN ; Van Etten RA ; Alroy J ; Durand JB ; Force T Cardiotoxicity of the cancer therapeutic agent imatinib mesylate. Nat. Med 2006, 12, 908–916.16862153

(33). Budman DR ; Calabro A ; Kreis W In vitro effects of dexrazoxane (Zinecard) and classical acute leukemia therapy: time to consider expanded clinical trials? Leukemia 2001, 15, 1517–1520.11587208

(34). Hasinoff BB ; Schnabl KL ; Marusak RA ; Patel D ; Huebner E Dexrazoxane (ICRF-187) protects cardiac myocytes against doxorubicin by preventing damage to mitochondria. Cardiovasc. Toxicol 2003, 3, 89–99.14501028

(35). Sepe DM ; Ginsberg JP ; Balis FM Dexrazoxane as a Cardioprotectant in Children Receiving Anthracyclines. Oncologist 2010, 15, 1220–1226.21051660

(36). Chang WT ; Yu D ; Lai YC ; Lin KY ; Liau I Characterization of the Mechanodynamic Response of Cardiomyocytes with Atomic Force Microscopy. Anal. Chem 2013, 85, 1395–1400.23265281

(37). Lieber SC ; Aubry N ; Pain J ; Diaz G ; Kim S-J ; Vatner SF Aging increases stiffness of cardiac myocytes measured by atomic force microscopy nanoindentation. Am. J. Physiol.: Heart Circ. Physiol 2004, 287, H645–H651.15044193

(38). Bongiorno T ; Kazlow J ; Mezencev R ; Griffiths S ; Olivares-Navarrete R ; McDonald JF ; Schwartz Z ; Boyan BD ; McDevitt TC ; Sulchek T Mechanical stiffness as an improved single-cell indicator of osteoblastic human mesenchymal stem cell differentiation. J. Biomech 2014, 47, 2197–2204.24296276

(39). Borbély A ; van der Velden J ; Papp Z ; Bronzwaer JGF ; Edes I ; Stienen GJM ; Paulus WJ Cardiomyocyte Stiffness in Diastolic Heart Failure. Circulation 2005, 111, 774–781.15699264

(40). Hund TJ ; Koval OM ; Li JD ; Wright PJ ; Qian L ; Snyder JS ; Gudmundsson H ; Kline CF ; Davidson NP ; Cardona N ; Rasband MN ; Anderson ME ; Mohler PJ A beta(IV)-spectrin/CaMKII signaling complex is essential for membrane excitability in mice. J. Clin. Invest 2010, 120, 3508–3519.20877009

(41). Jia YL ; Chen K ; Lin PH ; Lieber G ; Nishi M ; Yan R ; Wang Z ; Yao Y ; Li Y ; Whitson BA ; Duann P ; Li HC ; Zhou XY ; Zhu H ; Takeshima H ; Hunter JC ; McLeod RL ; Weisleder N ; Zeng CY ; Ma JJ Treatment of acute lung injury by targeting MG53-mediated cell membrane repair. Nat. Commun 2014, 5, 4387.25034454

(42). Wen JH ; Vincent LG ; Fuhrmann A ; Choi YS ; Hribar KC ; Taylor-Weiner H ; Chen S ; Engler AJ Interplay of matrix stiffness and protein tethering in stem cell differentiation. Nat. Mater 2014, 13, 979–987.25108614

(43). Hong TT ; Yang HH ; Zhang SS ; Cho HC ; Kalashnikova M ; Sun BM ; Zhang H ; Bhargava A ; Grabe M ; Olgin J ; Gorelik J ; Marban E ; Jan LY ; Shaw RM Cardiac BIN1 folds T-tubule membrane, controlling ion flux and limiting arrhythmia. Nat. Med 2014, 20, 624–632.24836577

(44). Katanosaka Y ; Iwasaki K ; Ujihara Y ; Takatsu S ; Nishitsuji K ; Kanagawa M ; Sudo A ; Toda T ; Katanosaka K ; Mohri S ; Naruse K TRPV2 is critical for the maintenance of cardiac structure and function in mice. Nat. Commun 2014, 5, 3932.24874017

(45). Cheng W ; Klauke N ; Sedgwick H ; Smith GL ; Cooper JM Metabolic monitoring of the electrically stimulated single heart cell within a microfluidic platform. Lab Chip 2006, 6, 1424–1431.17066165

(46). Tardiff JC Cardiac hypertrophy: stressing out the heart. J. Clin. Invest 2006, 116, 1467–1470.16741569

(47). Wang Y-X ; Korth M Effects of Doxorubicin on Excitation-Contraction Coupling in Guinea Pig Ventricular Myocardium. Circ. Res 1995, 76, 645–653.7895338

(48). Olson RD ; Mushlin PS ; Brenner DE ; Fleischer S ; Cusack BJ ; Chang BK ; Boucek RJ Doxorubicin cardiotoxicity may be caused by its metabolite, doxorubicinol. Proc. Natl. Acad. Sci. U. S. A 1988, 85, 3585–3589.2897122

(49). Herman EH ; Ferrans VJ ; Young RSK ; Hamlin RL Pretreatment with ICRF-187 allows a marked increase in the total cumulative dose of doxorubicin tolerated by beagle dogs. Drug Exp. Clin. Res 1988, 14, 563–570.

(50). Herman EH ; Hasinoff BB ; Steiner R ; Lipshultz SE A review of the preclinical development of dexrazoxane. Progress in Pediatric Cardiology 2014, 36, 33–38.

(51). Langer SW Dexrazoxane for the treatment of chemotherapy-related side effects. Cancer Manage. Res 2014, 6, 357–63.

(52). Barer R Refractometry and interferometry of living cells. J. Opt. Soc. Am 1957, 47, 545–556.13429433

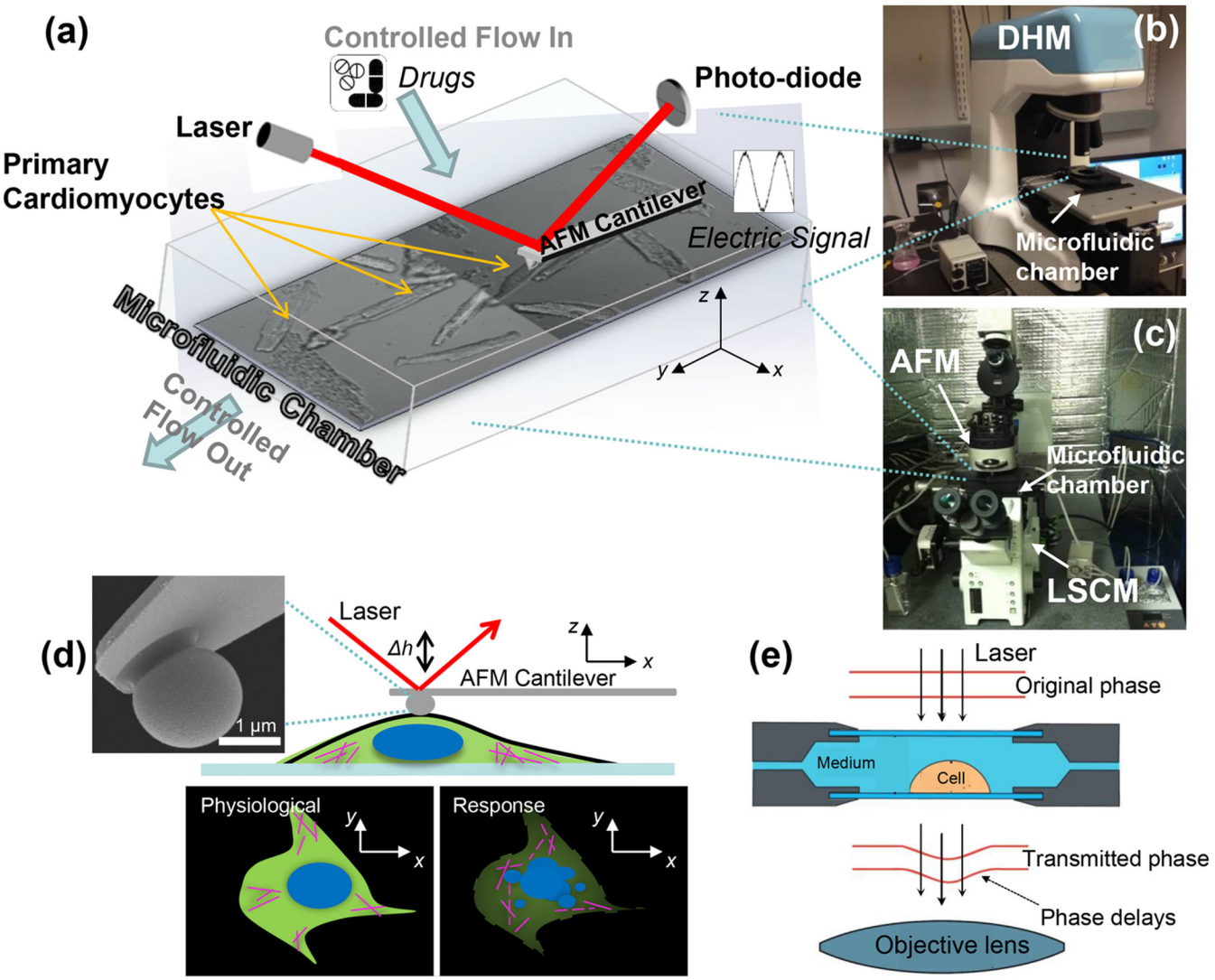

Figure 1.

Combined DHM (digital holographic microscope), AFM (atomic force microscope), and LSCM (laser scanning confocal microscope) nanoinstrumentation platform embedded with a microfluidic chamber for probing mechanics and mechanical properties of single cardiomyocytes in response to drug exposures. (a) Schematic drawing of the microfluidic chamber used to control the microenvironment during characterization. (b) DHM integrating with the microfluidic chamber. (c) Integrated AFM and LSCM where the microfluidic chamber sits between the two instruments. (d) Schematic drawing of AFM contact characterization on a single cell by a sphere tip cantilever. (e) Schematic drawing of DHM noncontact measurement principle. Quantitative phase images are obtained by comparing the transmitted phase with the original phase.

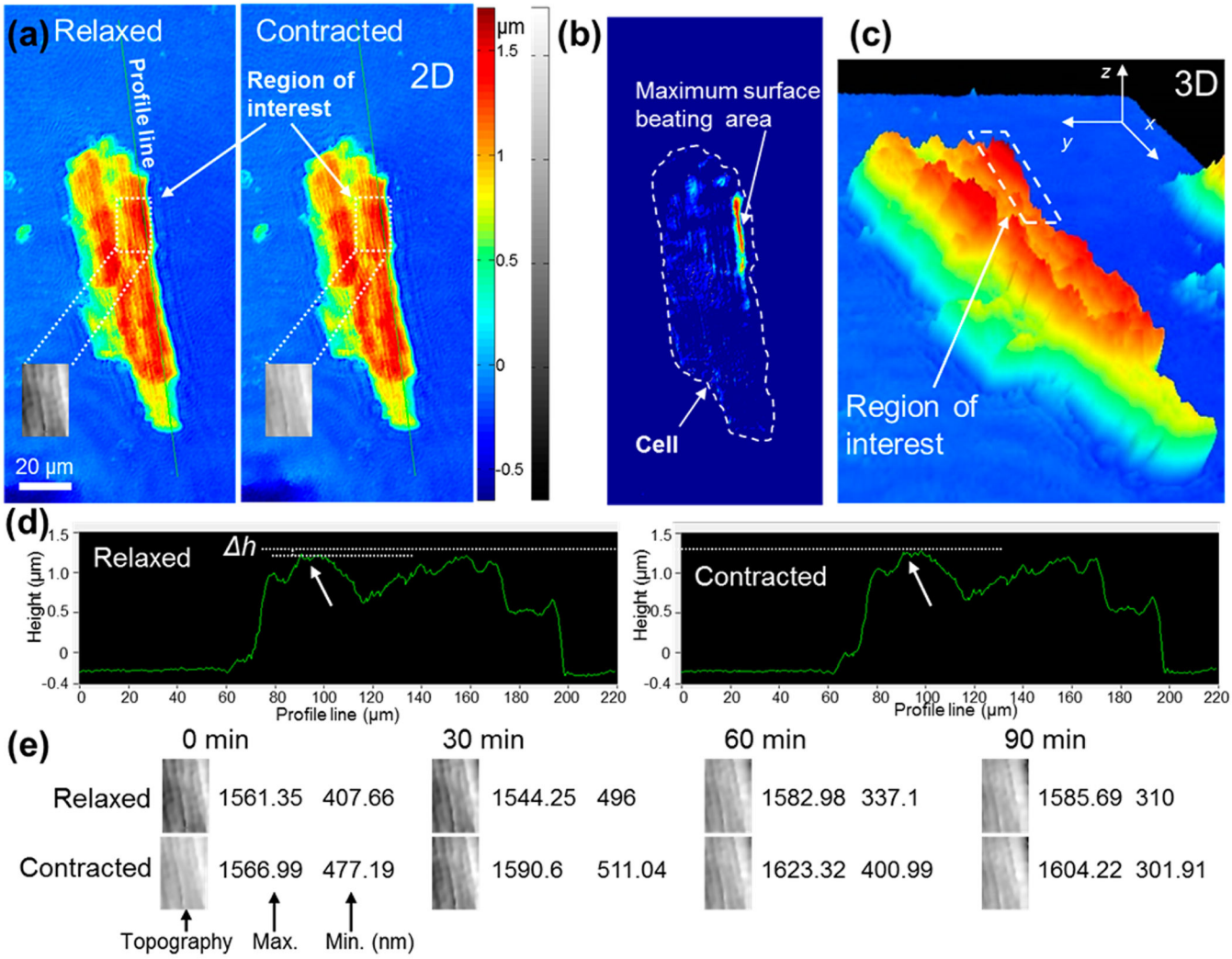

Figure 2.

DHM measurement of cell surface height changes during each contraction based on quantitative phase images in real time. (a) 2D phase images of a cardiomyocyte under relaxed and contracted statuses. Color indicates the phase differences and here can be considered as the cell thickness. Two profile lines are marked. (b) Maximum surface beating area used to define the region of interest (ROI). (c) 3D phase image which shows clear cell morphological information. (d) Phase profile data of the profile lines in panel a, which can be used to calculate the height change Δ*h* during the contraction. (e) Representative time-course data of the ROI marked in panel a to calculate the surface changes, including the maximum and minimum height points in a 2D region, cover the area around the contraction center.

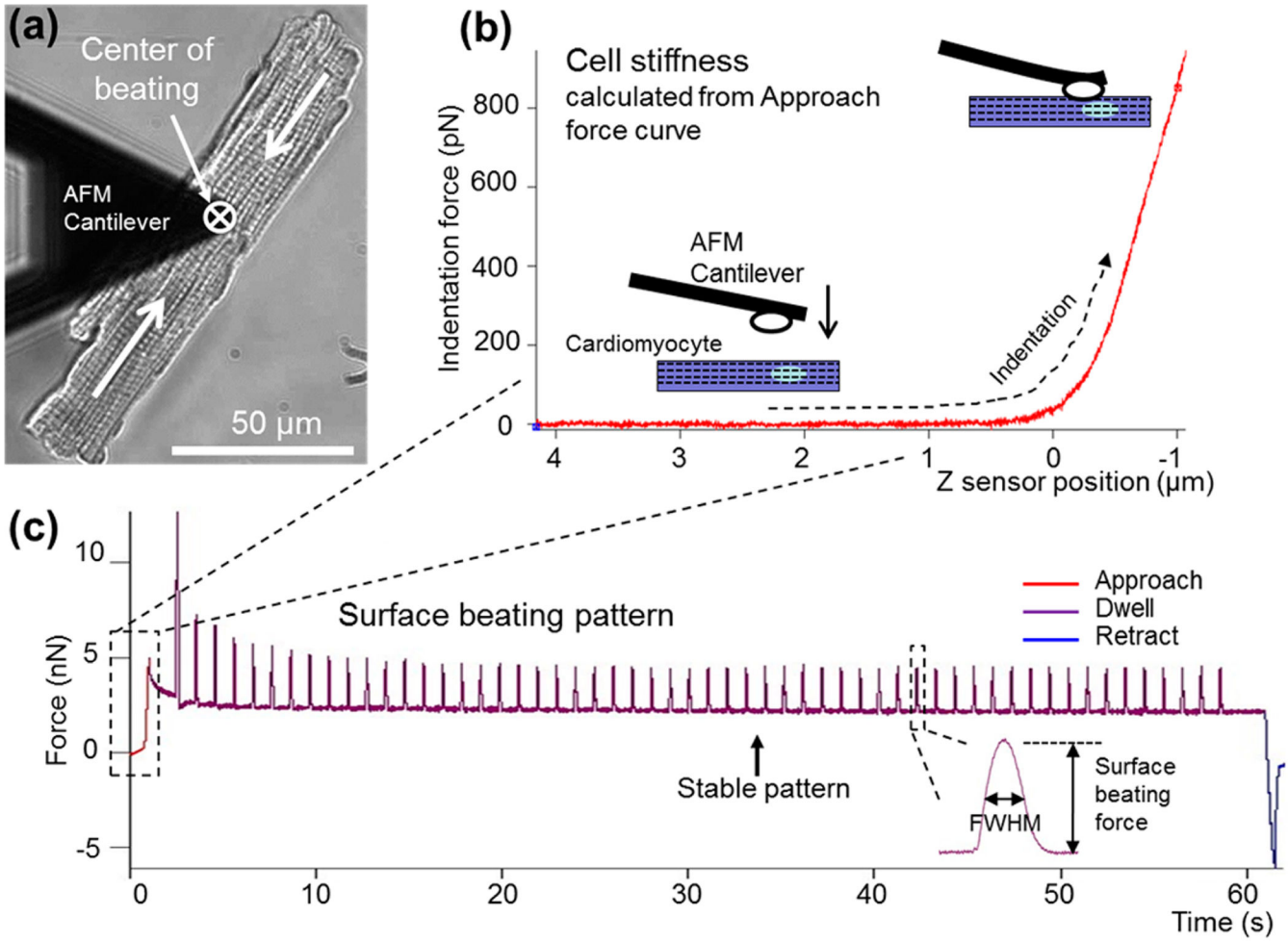

Figure 3.

AFM measurement using optimized protocol. (a) AFM cantilever alignment and positioning on the center of beating. (b) Cell stiffness data collected from the initial contact (approach) portion of the dwell curve. (c) Full dwell curve demonstrating where cell stiffness and beating dynamics (surface beating force and beating duration fwhm) were extracted.

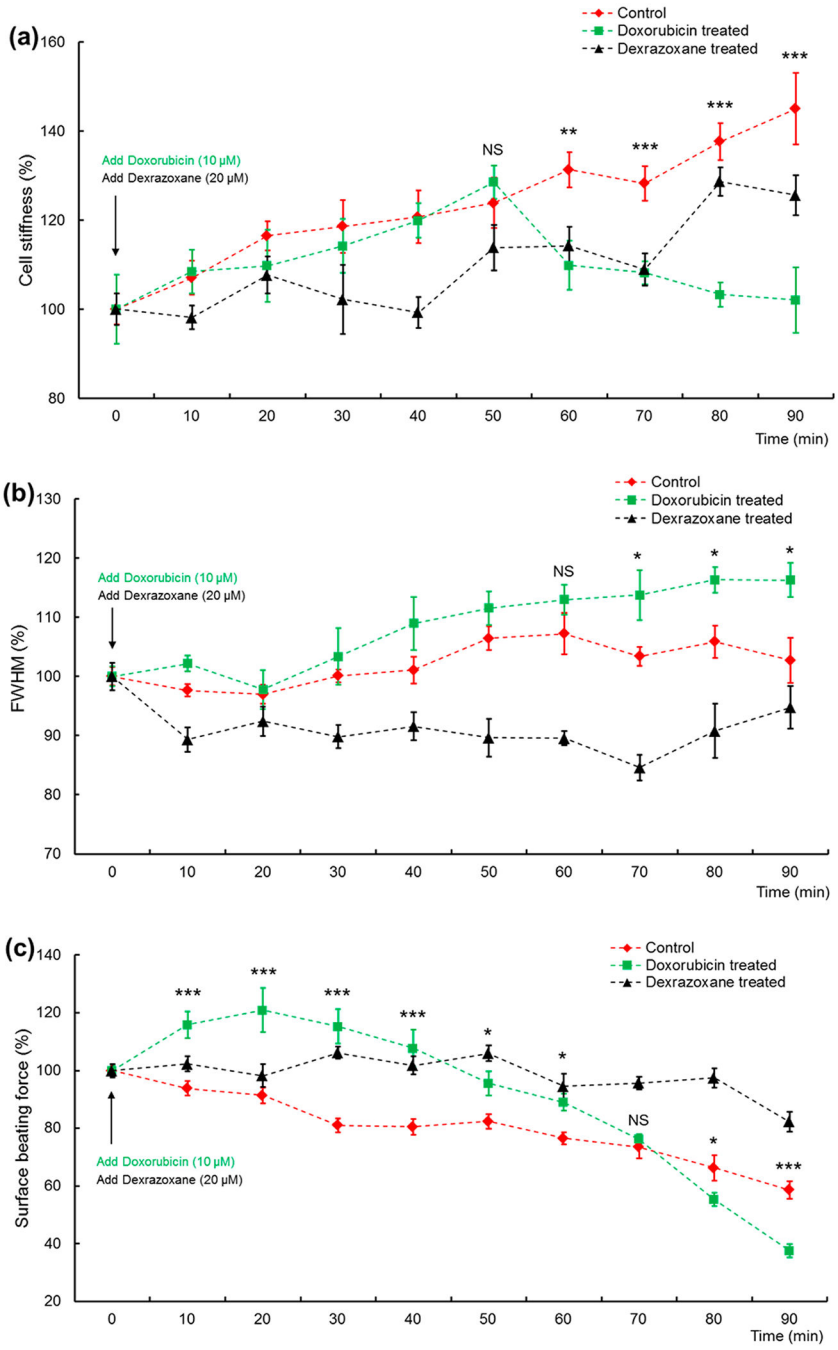

Figure 4.

Single drug-induced effects. All data are presented as the mean ± sem. Sample number n = 12. NS, not significant; *, $P < 0.05$; **, $P < 0.01$; ***, $P < 0.001$. (a) Stiffness versus time. The control group had a gradually increased stiffness while the doxorubicin treated ones had a lower value. The dexrazoxane treated ones had a small decrease at about 40 min and then showed almost the same changing trend as the control, with slightly lower value. Comparison between the control and doxorubicin treated groups from 50 to 90 min was performed. (b) fwhm versus time. Control samples had a relatively stable of fwhm with

small vibration during 70–80 min fwhm of doxorubicin treated samples increased gradually after about 30 min and finally reached to 15% higher than the control. fwhm of dexrazoxane treated samples decreased in the first 10 min and then maintained a significantly lower level than the control. Comparison between the control and doxorubicin treated groups from 60 to 90 min was performed. Additionally, between the control and dexrazoxane treated groups, significant difference was shown from 30 to 80 min ($P < 0.05$). (c) Surface beating force versus time. Doxorubicin treated cells had a beating peak up to 120% of the original level, lasting for 30 min, and a faster force decrease after 70 min. Dexrazoxane treated samples showed better beating capability and longer activities than control and doxorubicin treated cells. Comparison between the control and doxorubicin treated groups from 10 to 90 min was performed. Additionally, between the control and dexrazoxane treated groups, significant difference was shown from 30 to 90 min ($P < 0.01$).

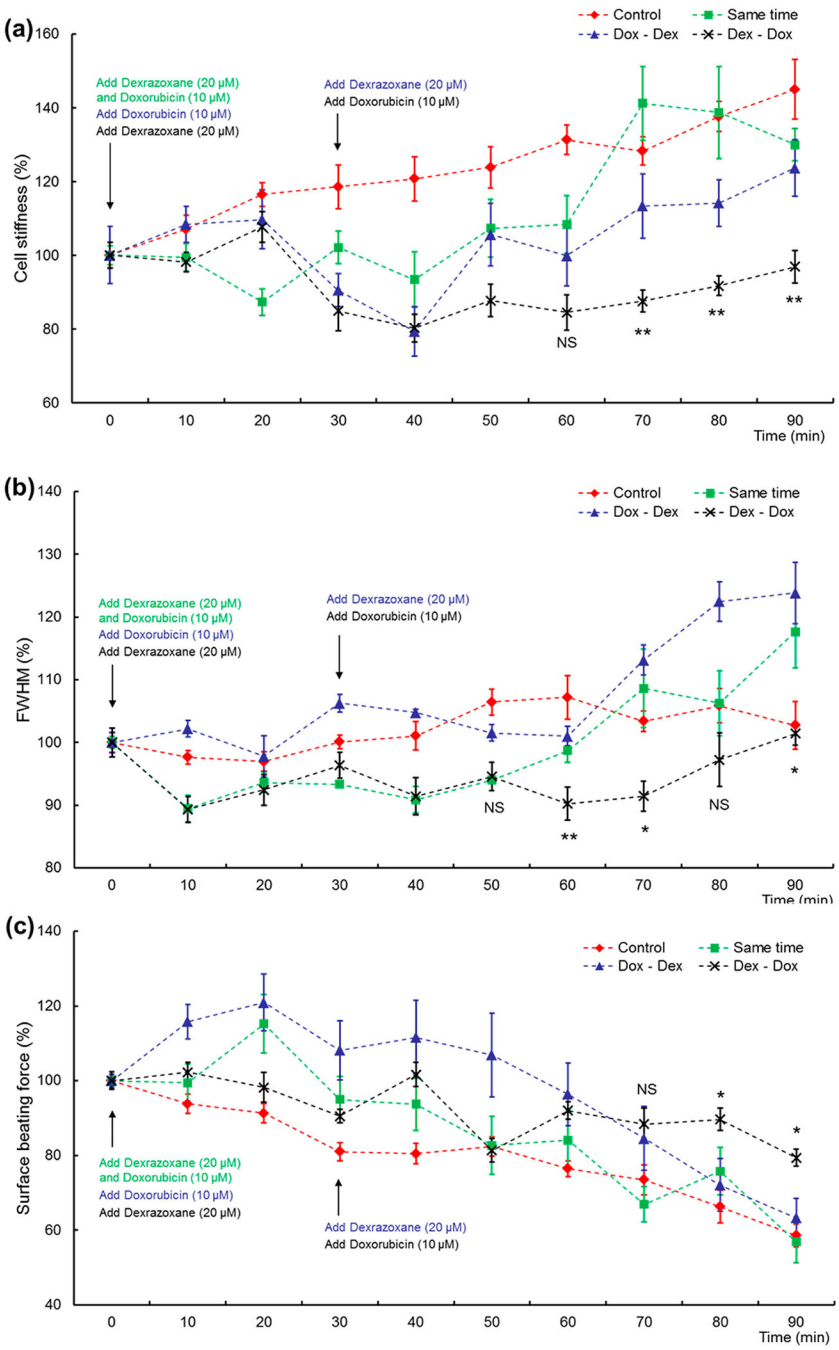

Figure 5.

Drug-combined effects. All data are presented as the mean ± sem. Sample number $n = 12$. NS, not significant; *, $P < 0.05$; **, $P < 0.01$. (a) Stiffness versus time. “Dex–Dox” group had a significantly lower value in comparison with other groups. Comparison between “Dox–Dex” and “Dex–Dox” groups from 60 to 90 min was performed. Additionally, Dex–Dox group had significant difference from 60 to 90 min ($P < 0.01$) in comparison with the control and “same time” groups. (b) fwhm versus time. After 50 min, the preadministration of the dexrazoxane group had a lower fwhm than other drug treated groups. It increased after

70 min and reached almost the same value as the control at the end of the experiments. Comparison between Dex–Dox and same time groups from 50 to 90 min was performed. Additionally, the Dex–Dox group had a significant difference from 40 to 90 min ($P < 0.01$) in comparison with the Dox–Dex group. (c) Force versus time. The preadministration of dexrazoxane group had the highest value of beating force at the end of the experiments. Comparison between Dox–Dex and Dex–Dox groups from 70 to 90 min was performed. Additionally, the Dex–Dox group had a significant difference from 70 to 90 min ($P < 0.05$) in comparison with control and same time groups.